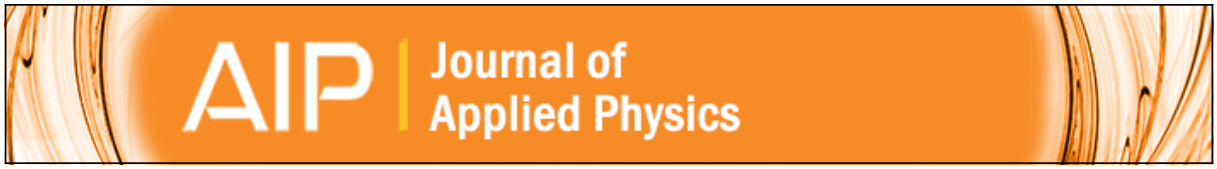

An analytical model to predict curvature effects of the carbon nanotube on the overall behavior of nanocomposites

B. J. Yang, H. Souri, Sunghwan Kim, Seunghwa Ryu, and H. K. Lee

Citation: Journal of Applied Physics **116**, 033511 (2014); doi: 10.1063/1.4890519
View online: http://dx.doi.org/10.1063/1.4890519
View Table of Contents: http://scitation.aip.org/content/aip/journal/jap/116/3?ver=pdfcov
Published by the AIP Publishing

Articles you may be interested in

Prediction of reinforcement degree for nanocomposites polymer/carbon nanotubes
AIP Conf. Proc. **1459**, 335 (2012); 10.1063/1.4738488

Dynamic mechanical behavior of magnetorheological nanocomposites filled with carbon nanotubes
Appl. Phys. Lett. **99**, 131912 (2011); 10.1063/1.3645627

Supersensitive linear piezoresistive property in carbon nanotubessilicone rubber nanocomposites
J. Appl. Phys. **104**, 024114 (2008); 10.1063/1.2956605

Modified Eshelby tensor modeling for elastic property prediction of carbon nanotube reinforced ceramic nanocomposites
Appl. Phys. Lett. **91**, 031903 (2007); 10.1063/1.2756360

Effect of nanorope waviness on the effective moduli of nanotube sheets
J. Appl. Phys. **95**, 5027 (2004); 10.1063/1.1687989

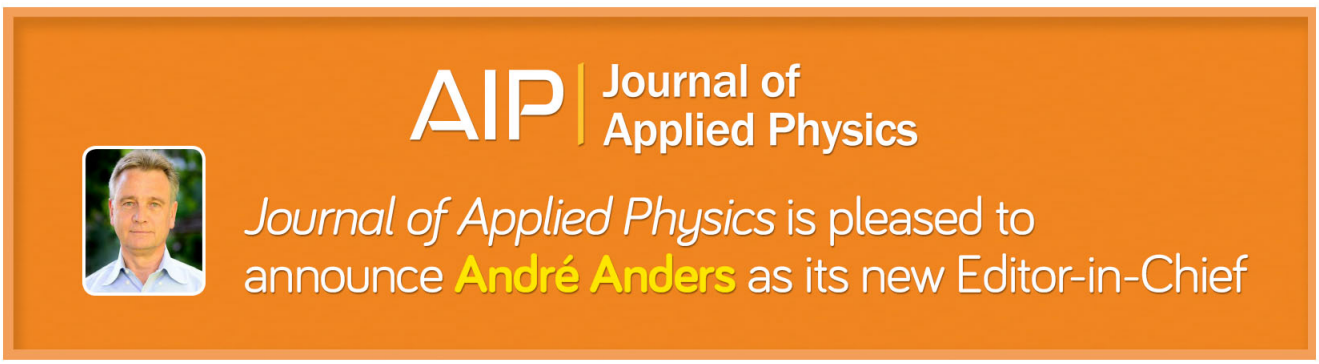

[This article is copyrighted as indicated in the article. Reuse of AIP content is subject to the terms at: http://scitation.aip.org/termsconditions. Downloaded to] IP: 143.248.122.51 On: Fri, 18 Jul 2014 14:27:21

An analytical model to predict curvature effects of the carbon nanotube on the overall behavior of nanocomposites

B. J. Yang,[1] H. Souri,[1] Sunghwan Kim,[2] Seunghwa Ryu,[2] and H. K. Lee[1,a)]
[1]*Department of Civil and Environmental Engineering, Korea Advanced Institute of Science and Technology (KAIST), 291 Daehak-ro, Yuseong-gu, Daejeon 305-701, South Korea*
[2]*Department of Mechanical Engineering, Korea Advanced Institute of Science and Technology (KAIST), 291 Daehak-ro, Yuseong-gu, Daejeon 305-701, South Korea*

(Received 23 May 2014; accepted 7 July 2014; published online 18 July 2014)

In this study, analytical expressions are introduced to provide a better understanding of carbon nanotubes (CNTs) curvature on the overall behavior of nanocomposites. The curviness of CNT is modeled as the wave geometries, and the transformed physical characteristics are applied to micromechanical framework. Since five independent elastic constants of CNTs are essential to derive the waviness effect, atomistic molecular statics simulations with varying nanotube radii are conducted. Influences of CNT curviness on the effective stiffness of the nanocomposites are analyzed, noting that the curvature effect is significantly influential on the effective stiffness of the nanocomposites, and it may improve or reduce the reinforcing effect depending on the orientation of CNTs. In addition, the predictions are compared with experimental data of the CNT-reinforced nanocomposites to assess the reliability of the proposed method. The developed constitutive model is expected to be used to determine the volume concentration of the reinforcing CNTs and mechanical responses of CNT-reinforced composites under various CNT curvature, radius, and orientation conditions. © *2014 AIP Publishing LLC*. [http://dx.doi.org/10.1063/1.4890519]

I. INTRODUCTION

Carbon nanotubes (CNTs) have been employed as one of the most popular reinforcements within polymeric or cementitious composites due to their superior mechanical properties including high elastic modulus and tensile strength.[1,2] However, although the physical characteristics of the nanotube are extraordinary, the CNT-reinforced nanocomposites often display limited improvements in stiffness. Various issues have thus been raised regarding their reinforcing efficiency in association with the shape,[3,4] the debonding damage,[5,6] the dispersion,[7] and an orientation of CNTs.[2]

Numerous attempts have been made in accordance with the reinforcing effect of CNTs on the overall behavior of nanocomposite materials. Fisher *et al.*[3] investigated the effect of CNT waviness on the effective stiffness by employing both the finite element method (FEM) and the Mori-Tanaka scheme.[3] Shao *et al.*[4] derived an approximate model to estimate the effect of partial debonding and CNT waviness on the composite system and concluded that the waviness of CNTs significantly reduces the stiffening effect of CNTs.[4] In addition, a micromechanical model for estimating the effective elastic moduli of CNT-reinforced composites and for considering the waviness and random orientation of nanotubes was proposed by Anumandla and Gibson.[8] This model was based on the traditional composite micromechanics and showed that the reinforcing effectiveness of CNTs decreases as the nanotube waviness increases.[8]

Moreover, some researchers have focused on modeling and on predicting the behavior of the nanocomposite by considering transverse isotropic characteristics of CNTs. To investigate the effect of CNTs, a series of molecular dynamics (MD) simulations were conducted[9] and showed that embedding the defective CNTs in polypropylene resulted in a smaller longitudinal Youngs modulus compared to nanocomposites with pristine CNTs.[9] In another study by Barai and Weng,[2] which was based on the Mori-Tanaka mean field approach, a two-scale micromechanics model was proposed to examine the effect of a CNT stiffness condition on nanocomposites. The predicted results showed that the presence of imperfect CNTs could severely reduce the stiffness and yield strength of the CNT-reinforced polymeric nanocomposite.[2]

In this paper, a combined molecular statics (MS) simulations and micromechanics-based model for CNT-reinforced nanocomposites is derived.[10] Particularly, a constitutive equation of CNT-reinforced composites with the effects of curviness and an inclusion orientation is developed.[11,12] Since five independent elastic moduli of the transversely isotropic CNTs are essential to derive the curvature effect,[9] atomistic simulations with varying nanotube radii are carried out. The predicted MS results are then applied to the developed framework.

Consequently, influences of the CNT curviness on the effective stiffness of the nanocomposites are theoretically examined via numerical tests. It reveals that the curvature effect is significantly influential on the overall behavior of the nanocomposites, and it may improve or reduce the reinforcing effect depending on the orientation of CNTs. The comparative study between the developed model and experimental result[13] is also considered, indicating that the proposed method can be utilized to predict the stiffening capacity of CNTs under different curvature and orientation conditions.

a)Electronic mail: leeh@kaist.ac.kr

 © 2014 AIP Publishing LLC

[This article is copyrighted as indicated in the article. Reuse of AIP content is subject to the terms at: http://scitation.aip.org/termsconditions. Downloaded to] IP: 143.248.122.51 On: Fri, 18 Jul 2014 14:27:21

II. EFFECTS OF CURVINESS ON THE ELASTIC PROPERTIES OF CNTs

We first consider that the CNTs have difficulty in maintaining their straight shape when CNTs are distributed through the matrix material, as shown in Fig. 1(a). To consider the curviness effect on the physical characteristics of CNTs, an analytical theory is adopted here.[14] As shown in Fig. 1(b), the curviness of the ellipsoidal inclusions is characterized by the waviness factor $\omega = A/L$,[14,15] and it can be modeled using the mathematical descriptions of the wave geometries as follows:[14]

$$\begin{aligned}\tilde{\mathbf{C}}_1(\omega) &= \frac{1}{L}\int_0^L \tau_{ip}\tau_{jq}\tau_{kr}\tau_{ls}\mathbf{C}_1 \mathrm{d}x, \\ &= \tilde{\lambda}_{IK}\delta_{ij}\delta_{kl} + \tilde{\mu}_{IJ}\left(\delta_{ik}\delta_{jl} + \delta_{il}\delta_{jk}\right),\end{aligned} \tag{1}$$

where $\mathbf{C}_1$ signifies the transversely isotropic stiffness tensor of straight CNTs and τ_{ij} is the direction cosine.[14] $\tilde{\lambda}_{IK}$ and $\tilde{\mu}_{IJ}$ can be explicitly derived after carrying out the lengthy algebra, and the components are given as[15]

$$\begin{aligned}\tilde{\lambda}_{11} &= I_1(c_{11} - c_{22}) + c_{22}, \\ \tilde{\lambda}_{12} &= I_2(c_{11} - 2c_{12} + c_{22} - 4c_{66}) + c_{12}, \\ \tilde{\lambda}_{13} &= (I_1 + I_2)(c_{12} - c_{23}) + c_{23}, \\ \tilde{\lambda}_{22} &= I_1(c_{22} - c_{11}) + c_{11}, \\ \tilde{\lambda}_{23} &= (I_1 + I_2)(c_{23} - c_{12}) + c_{12}, \\ \tilde{\lambda}_{21} &= \tilde{\lambda}_{12}, \quad \tilde{\lambda}_{31} = \tilde{\lambda}_{13}, \quad \tilde{\lambda}_{32} = \tilde{\lambda}_{23}, \quad \tilde{\lambda}_{33} = c_{33},\end{aligned} \tag{2}$$

and

$$\begin{aligned}\tilde{\mu}_{11} &= I_2(c_{12} - c_{22} + 2c_{66}), \\ \tilde{\mu}_{12} &= I_2(c_{11} - 2c_{12} + c_{22} - 4c_{66}) + c_{66}, \\ \tilde{\mu}_{13} &= (I_1 + I_2)(c_{66} - c_{44}) + c_{44}, \\ \tilde{\mu}_{22} &= I_2(c_{12} + 2c_{66} - c_{11}), \\ \tilde{\mu}_{23} &= (I_1 + I_2)(c_{44} + c_{66}), \quad \text{Other} = 0,\end{aligned} \tag{3}$$

in which

$$I_1 = \frac{1 + 2\pi^2\omega^2}{(1 + 4\pi^2\omega^2)^{1.5}}, \quad I_2 = \frac{2\pi^2\omega^2}{(1 + 4\pi^2\omega^2)^{1.5}}, \tag{4}$$

and

$$\begin{aligned}c_{11} &= \frac{E_L^2(\nu_{23} - 1)}{E_L(\nu_{23} - 1) + 2E_T\nu_{12}^2}, \\ c_{12} &= \frac{E_L E_T \nu_{12}}{E_L - E_L\nu_{23} - 2E_T\nu_{12}^2}, \\ c_{22} &= \frac{E_T(-E_L + E_T + \nu_{12}^2}{(\nu_{23} + 1)\left[E_L(\nu_{23} - 1) + 2E_T\nu_{23}^2\right]}, \\ c_{23} &= \frac{-E_T\left(E_L\nu_{23} + E_T\nu_{12}^2\right)}{(\nu_{23} + 1)\left[E_L(\nu_{23} - 1) + 2E_T\nu_{12}^2\right]}, \\ c_{33} &= c_{22}, \quad c_{44} = \mu_T, \quad c_{66} = \mu_L,\end{aligned} \tag{5}$$

where $\omega = A/L$ (see Fig. 1), the components E_L, E_T, μ_T, μ_L, and ν_{12} are calculated via the MS simulations (Table I) and $\nu_{23} = E_T/2\mu_T - 1$.

The transversely isotropic stiffness tensor of straight CNTs ($\mathbf{C}_1$) is characterized by five independent elastic constants: longitudinal Young's and shear modulus (E_L, μ_L), transverse Young's and shear modulus (E_T, μ_T), and the Poisson's ratio in the 1–2 direction (ν_{12}). Since an experimentally measurement of the elastic constants would be enormously complicated, the coefficients are obtained by the MS simulations.

The atomistic properties of CNTs can be ideally described by the MS simulation, and thus the proposed method would be useful in reflecting the physical nature of the CNTs.[6] The MS simulations are carried out by using Large-scale Atomistic Modeling Massively Parallelized Simulation (LAMMPS) code.[16] Four different zigzag types of CNTs are considered for the MS simulations with respect to the CNT chiral vector from (10,0) to (25,0), as shown in Fig. 2. The adaptive intermolecular reactive empirical bond order (AIREBO) potential[17,18] is adopted here to describe the interatomic potential of carbon, and the effective wall thickness of CNTs is set to $t = 0.334$ nm.[19]

The details of calculating the five independent elastic constants of the CNTs are addressed as follows. E_L and ν_{12} are estimated from the uniaxial tension simulation along the 11 direction.[9] It is noted that all tensile deformations are performed with a small amount of strain ($-0.2\%\sim0.2\%$) to consider only elastic deformation region. Then, the deformation energy density from the results is fit to a second-order function of the engineering longitudinal strain.[9] E_T is obtained from the relations between the deformation energy density and the transverse strain. μ_L and μ_T are obtained from a torsional deformation along the 11 direction and shear along

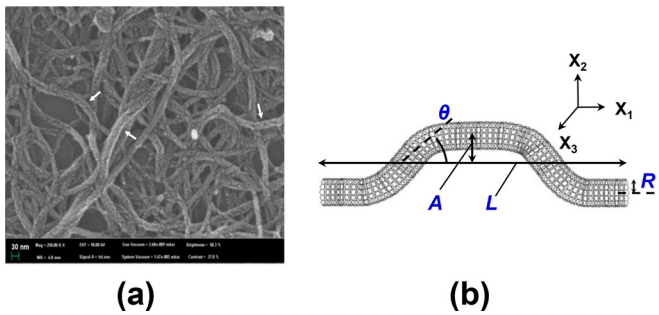

FIG. 1. (a) SEM image of randomly oriented and curved CNTs embedded in the matrix material and (b) an illustrative schematic of nanotube curviness in this study.

TABLE I. Predicted elastic constants of CNT with varying chiralities of the nanotube obtained by MS simulations (R: radius, E_L: longitudinal Young's modulus, E_T: transverse Young's modulus, μ_L: longitudinal shear modulus, μ_T: transverse shear modulus, and ν_{12}: the Poisson's ratio in the 1–2 direction).

Elastic constants	(10,0)	(15,0)	(20,0)	(25,0)
R (nm)	0.39	0.59	0.78	0.98
E_L (GPa)	1049.70	975.65	928.37	899.59
E_T (GPa)	185.04	268.86	354.06	439.86
μ_L (GPa)	353.41	306.30	292.48	290.02
μ_T (GPa)	158.74	151.52	148.86	147.57
ν_{12}	0.17	0.25	0.29	0.31

[This article is copyrighted as indicated in the article. Reuse of AIP content is subject to the terms at: http://scitation.aip.org/termsconditions. Downloaded to] IP: 143.248.122.51 On: Fri, 18 Jul 2014 14:27:21

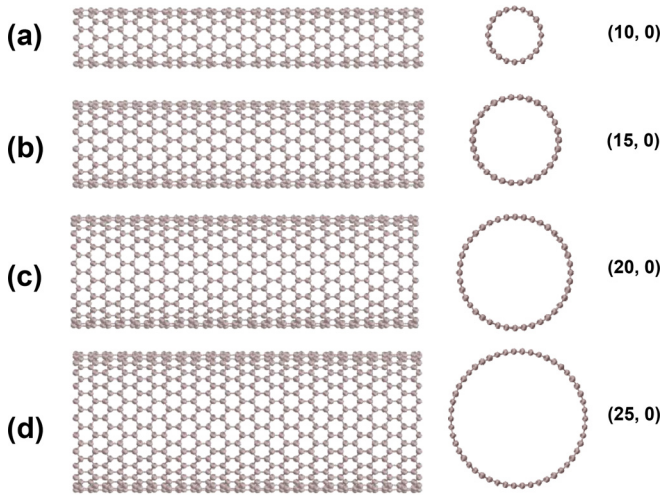

FIG. 2. Atomistic structures of CNTs with varying chiral vector: (a) (10, 0), (b) (15, 0), (c) (20, 0), and (d) (25, 0).

the two transverse directions, respectively.[9] The obtained elastic constants of CNTs by MS simulations are summarized in Fig. 3 and Table I.

III. EFFECTIVE STIFFNESS TENSOR OF NANOCOMPOSITES CONTAINING ALIGNED AND 3D RANDOMLY ORIENTED CNTs

The effective elastic modulus of nanocomposites composed of a matrix material (phase 0) and CNTs aligned in X_1 axis direction (phase 1) can be estimated through a micromechanical approach for homogenization.[20,21] By accounting for the ensemble volume averaged method, the effective elasticity tensor for two-phase composites can be determined as follows:[20,22]

$$\mathbf{C}^* = \mathbf{C}_0 \cdot \left[\mathbf{I} + \left\{ \begin{matrix} \phi_1 (\mathbf{A}_1 + \mathbf{S})^{-1} \cdot \\ [\mathbf{I} - \phi_1 \mathbf{S} \cdot (\mathbf{A}_1 + \mathbf{S})^{-1}]^{-1} \end{matrix} \right\} \right], \tag{6}$$

with

$$\mathbf{A}_1 = [\tilde{\mathbf{C}}_1(\omega) - \mathbf{C}_0]^{-1} \cdot \mathbf{C}_0, \tag{7}$$

where $\mathbf{C}_0$ and $\mathbf{I}$ are the stiffness tensor of the matrix material and the fourth-rank identical tensor, respectively. In addition,

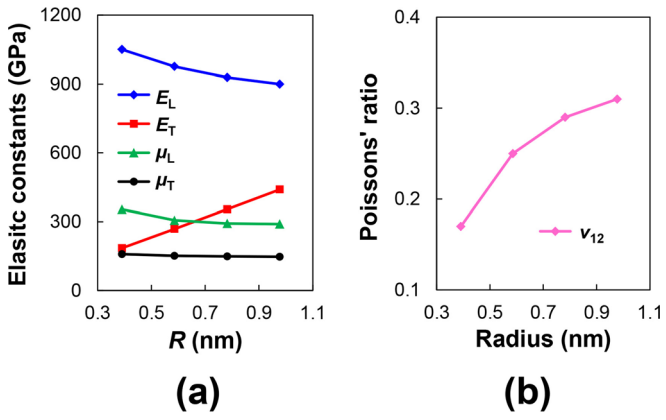

FIG. 3. The predicted (a) elastic constants and (b) the Poisson's ratio of CNTs from MS simulations.

ϕ_1 is the volume fraction of CNTs and $\mathbf{S}$ signifies Eshelby's tensor, which is given as[23]

$$S_{ijkl} = \frac{1}{4(1-\nu_0)} \left[\begin{matrix} S_{IK}^{(1)} \delta_{ij}\delta_{kl} + \\ S_{IJ}^{(2)} \left(\delta_{ik}\delta_{jl} + \delta_{il}\delta_{jk}\right) \end{matrix} \right], \tag{8}$$

where the parameters $S_{IK}^{(1)}$ and $S_{IJ}^{(2)}$ are listed in Appendix A. The stiffness tensor of CNTs with curvature effects $\tilde{\mathbf{C}}_1(\omega)$ can be obtained by combining Eq. (1) and MS simulation results.[15]

Hence, the effective elastic constitutive tensor of the curved and aligned CNTs-reinforced nanocomposites rendered by Eq. (6) is

$$\mathbf{C}^* = C_{IK}^{(1)} \delta_{ij}\delta_{kl} + C_{IJ}^{(2)} (\delta_{ik}\delta_{jl} + \delta_{il}\delta_{jk}), \tag{9}$$

with

$$\begin{aligned} C_{IK}^{(1)} &= 2\lambda_0 \left(\chi_{KK}^{(2)} + \frac{1}{2} \right) + 2\mu_0 \chi_{IK}^{(1)} + \lambda_0 \sum_{Q=1}^{3} \chi_{QK}^{(1)}, \\ C_{IJ}^{(2)} &= 2\mu_0 \left(\chi_{IJ}^{(2)} + \frac{1}{2} \right), \end{aligned} \tag{10}$$

where λ_0 and μ_0 signify the Lamé constants of the matrix material, δ_{ij} denotes the Kronecker delta, and the parameters $\chi_{IK}^{(1)}$ and $\chi_{IJ}^{(2)}$ are listed in Appendix B.[14]

Furthermore, the 3D randomly orientated distribution of CNTs can be described as[24]

$$\langle \mathbf{C}^* \rangle = \frac{\int_{-\pi}^{\pi} \int_{0}^{\pi} \int_{0}^{\pi/2} \bar{\mathbf{C}}^*(\varsigma, \gamma, \psi) \sin\gamma \mathrm{d}\varsigma \mathrm{d}\gamma \mathrm{d}\psi}{\int_{-\pi}^{\pi} \int_{0}^{\pi} \int_{0}^{\pi/2} \sin\gamma \mathrm{d}\varsigma \mathrm{d}\gamma \mathrm{d}\psi}, \tag{11}$$

where $\langle \cdot \rangle$ denotes the 3D orientation average process[25] and $\bar{\mathbf{C}}^* = \tau_{ip}\tau_{jq}\tau_{kr}\tau_{ls}C^*_{pqrs}$. After lengthy but straightforward algebra, the effective elastic tensor of the curved and 3D randomly orientated CNTs-reinforced nanocomposites becomes[24]

$$\langle \mathbf{C}^* \rangle = \langle C_{IK}^{(1)} \rangle \delta_{ij}\delta_{kl} + \langle C_{IJ}^{(2)} \rangle (\delta_{ik}\delta_{jl} + \delta_{il}\delta_{jk}), \tag{12}$$

with

$$\langle C_{IK}^{(1)} \rangle = \frac{1}{15} \left[\begin{matrix} C_{11}^{(1)} + 4C_{12}^{(1)} + 4C_{21}^{(1)} + 6C_{22}^{(1)} \\ +2C_{11}^{(2)} - 4C_{12}^{(2)} + 2C_{22}^{(2)} \end{matrix} \right], \tag{13}$$

$$\langle C_{IJ}^{(2)} \rangle = \frac{1}{15} \left[\begin{matrix} C_{11}^{(1)} - C_{12}^{(1)} - C_{21}^{(1)} + C_{22}^{(1)} \\ +2C_{11}^{(2)} + 6C_{12}^{(2)} + 7C_{22}^{(2)} \end{matrix} \right], \tag{14}$$

where $C_{IK}^{(1)}$ and $C_{IJ}^{(2)}$ can be derived from Eq. (10).

IV. NUMERICAL SIMULATIONS AND EXPERIMENTAL COMPARISONS

A series of numerical simulations have been performed to explore the effects of the curvature on the CNTs-reinforced nanocomposites. We consider the CNT/propylene composites

[This article is copyrighted as indicated in the article. Reuse of AIP content is subject to the terms at: http://scitation.aip.org/termsconditions. Downloaded to] IP: 143.248.122.51 On: Fri, 18 Jul 2014 14:27:21

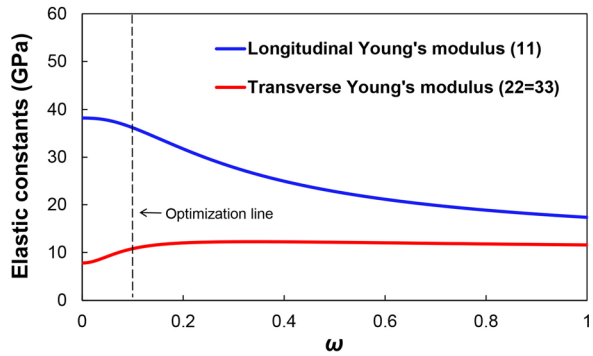

FIG. 4. The elastic properties of the aligned CNT-reinforced nanocomposites with respect to the CNT curvature.

for the numerical tests, and the constituent properties of the materials are as follows: $E_0 = 1.24\,\text{GPa}$ and $\nu_0 = 0.41$, where E_0 and ν_0 denote the Young's modulus and the Poisson's ratio of the matrix, respectively.[13] Based on the MS simulations, the transversely isotopic elastic constants of CNTs can be defined as exponential function of the nanotube radius given by $E_L = 1150.7\exp(-0.26R)$, $E_T = 108.5\exp(1.47R)$, $\mu_L = 387.2\exp(-0.33R)$, $\mu_T = 164.7\exp(-0.12R)$, and $\nu_{12} = 0.126\exp(R)$. The lower indexes L and T represent the longitudinal and transverse directions, respectively.

Fig. 4 shows the elastic constants of the aligned CNTs-reinforced propylene composites with respect to the waviness factor ($\omega = A/L$). In this simulation, the length, the radius, and the volume fraction of the CNTs are assumed as $L = 60\,\mu\text{m}$, $R = 12.5\,\text{nm}$, and $\phi_1 = 5\%$.[13] As shown in Fig. 4, the longitudinal Young's modulus of the nanocomposites decreases as the ω increases, while the transverse Young's modulus becomes stiffer as ω increases for aligned orientation case. The curviness effects in the transverse direction, however, begin to diminish when the ω exceeds 0.2.

The simulation results imply that if the orientation and the curviness of CNTs can be controllable, it would help to design better nanocomposites. When the nanocomposite contains aligned CNTs, the reinforcement effect is usually pronounced in the longitudinal direction. The present predictions, however, indicate that the stiffness in the transverse direction of nanocomposites can be improved by curving CNTs. To consider the correlation between the waviness factor ω and the overall stiffness of the nanocomposites, it is conjectured that $\omega = 0.1$ would be an optimized value to

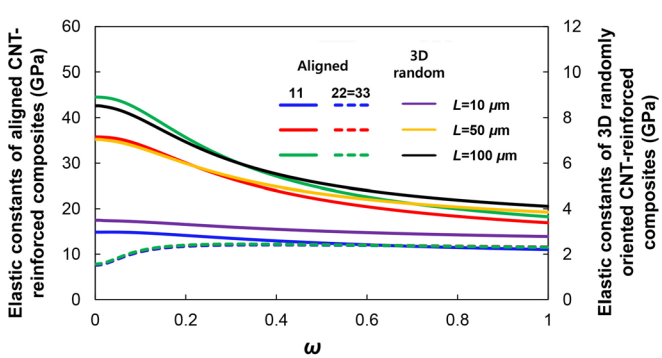

FIG. 5. The curvature effects of the aligned and 3D randomly oriented CNTs on the effective elastic constants of the nanocomposites.

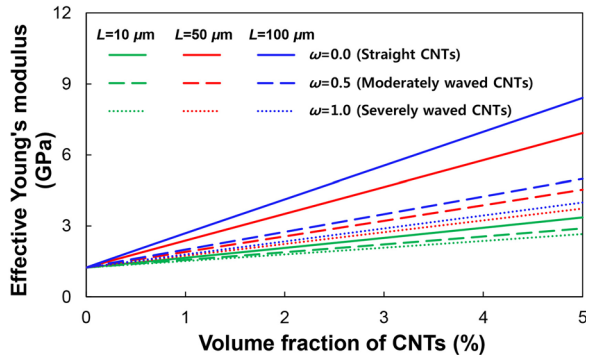

FIG. 6. The influences of the curvature and the length of CNTs on the effective Young's modulus of nanocomposites reinforced by 3D randomly oriented nanotubes.

achieve an enhanced transverse Young's modulus with a relatively small stiffness reduction in the longitudinal direction. Hence, $\omega = 0.1$ is assumed to be the optimization line in the present study, and the line is plotted in Fig. 4.

The curvature effects of the aligned and 3D randomly oriented CNTs on the effective elastic constants of the nanocomposites are plotted in Fig. 5. It shows that a smaller reinforcing effect is observed as the nanotube length decreases, whereas a stronger stiffening effect is predicted for the lengthier CNTs. It is also noted that the curvature effect becomes more pronounced as the length of the CNTs increases; however, considerably less influences are observed in the case of the transverse Young's modulus.

Fig. 6 displays the prediction results from the developed model with respect to the content variations of CNTs. In the present study, it is assumed that $\omega = 0.0$, 0.5, and 1.0 signify the straight, the moderately waved, and the severely curved CNTs, respectively. The CNT lengths used in the numerical simulations are $L = 10$, 50, and $100\,\mu\text{m}$, respectively. It is seen from Fig. 6 that the nanotube length significantly affects the overall stiffness of the nanocomposites, and the curvature effect becomes more pronounced as the length of the CNTs increases. Based on the simulation results, a stronger curvature effect of CNTs is noted for the lengthier CNTs.

In addition, we compared the present predictions with the available experimental data[13] to verify the predictive capability of the proposed model. Andrews *et al.*[13] conducted the experimental tests to characterize the effective Young's modulus of the nanocomposites for different volume fraction of the CNTs. The 3D randomly oriented CNT-reinforced propylene composite was experimentally investigated by Andrews *et al.*,[13] and the reported material properties of the matrix and the CNT are identical to the previously utilized values in numerical tests. Note that the average value of the CNT lengths reported in Andrews *et al.*[13] (20–100 m) is utilized here for experimental comparisons as: $L = 60\,\mu\text{m}$.[13] It should be emphasized that the only fitted model parameter to the experiment is the waviness factor, ω. Three different waviness factors ($\omega = 0.0$, 0.5, and 1.0) are, therefore, considered.

Fig. 7 shows that neglecting the curvature properties of the CNTs can cause an overestimation of the nanocomposite stiffness. However, the prediction that considers the curviness mechanisms leads to a reduction in the stiffening effect

[This article is copyrighted as indicated in the article. Reuse of AIP content is subject to the terms at: http://scitation.aip.org/termsconditions. Downloaded to] IP: 143.248.122.51 On: Fri, 18 Jul 2014 14:27:21

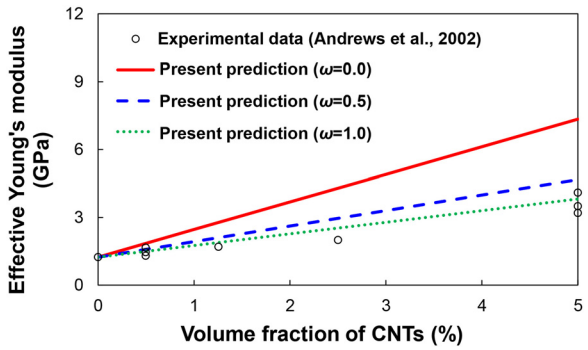

FIG. 7. The comparisons between the experimental data[13] and the present predictions for various CNT contents.

of the CNTs and results in an agreement between the experimental and theoretical results. The comparative agreement may demonstrate the predictive capacity of the proposed framework for the CNTs-reinforced composite systems.

V. CONCLUSIONS

In this work, the effects of the curvature and orientation of the CNTs are investigated theoretically using MS simulations and micromechanical approaches. Numerous parametric studies and experimental comparison are performed, and the important observations from the results are highlighted as follows:

(1) The MS simulations are conducted to calculate the transversely isotropic elastic constants of CNTs, resulting that the mechanical properties of CNTs are fairly dependent on the nanotube radius.
(2) The transverse Young's modulus of aligned CNTs-reinforced composites can be improved by curving CNTs; however, the curved CNTs exert a weakening effect to the longitudinal Young's modulus for nanocomposites containing aligned CNTs. It implies that if the orientation and the curviness of CNTs can be controllable, it would help to design better nanocomposites.
(3) For the nanocomposites reinforced by 3D randomly oriented CNTs, the effective stiffness of the composites decreases as the curviness increases. In addition, it is observed that the curvature effect is more influential as the nanotube length increases.
(4) The comparisons between the experimental results and the present predictions are included, and their agreement shows the predictive capability of the developed model.

The obtained findings indicate that the CNTs can provide an adequate reinforcement of the composites, and we expect that the proposed model will play a role in predicting the stiffening capacity of CNTs under various curvature and orientation cases.

ACKNOWLEDGMENTS

This research was sponsored by the National Research Foundation of Korea (NRF) grants funded by the Korea government (NRF-2012R1A2A4A01008855).

APPENDIX A: PARAMETERS OF ESHELBY'S TENSOR

The parameters $S_{IK}^{(1)}$ and $S_{IJ}^{(2)}$ can be expressed as[23]

$$\begin{aligned}
S_{11}^{(1)} &= 2\left[\frac{(2\nu_0-1)\alpha}{1+\alpha}+\frac{1}{3}\left\{1-\frac{1}{(1+\alpha)^2}\right\}\right],\\
S_{12}^{(1)} &= 2\left[\frac{\alpha^2}{(1+\alpha)^2}-\frac{(1-2\nu_0)\alpha}{\alpha+1}\right],\\
S_{13}^{(1)} &= \frac{4\nu_0\alpha}{1+\alpha},\quad S_{21}^{(1)} = 2\left[\frac{1}{(1+\alpha)^2}-\frac{1-2\nu_0}{\alpha+1}\right],\\
S_{22}^{(1)} &= 2\left[\frac{2\nu_0-1}{1+\alpha}+\frac{1}{3}\left\{1-\frac{\alpha^2}{(1+\alpha)^2}\right\}\right],\quad S_{23}^{(1)} = \frac{4\nu_0}{1+\alpha},\\
S_{31}^{(1)} &= S_{32}^{(1)} = S_{33}^{(1)} = 0,
\end{aligned} \tag{A1}$$

and

$$\begin{aligned}
S_{11}^{(2)} &= 2\left[\frac{(1-2\nu_0)\alpha}{1+\alpha}+\frac{1}{3}\left\{1-\frac{1}{(1+\alpha)^2}\right\}\right],\\
S_{12}^{(2)} &= 2\left[(1-\nu_0)-\frac{\alpha}{(\alpha+1)^2}\right],\\
S_{13}^{(2)} &= \frac{2(1-2\nu_0)\alpha}{1+\alpha},\quad S_{21}^{(2)} = S_{12}^{(2)},\\
S_{22}^{(2)} &= 2\left[\frac{1-2\nu_0}{1+\alpha}+\frac{1}{3}\left\{1-\frac{\alpha^2}{(1+\alpha)^2}\right\}\right],\quad S_{23}^{(2)} = \frac{2(1-\nu_0)}{1+\alpha},\\
S_{31}^{(2)} &= S_{13}^{(2)},\ S_{32}^{(2)} = S_{23}^{(2)},\ S_{31}^{(2)} = 0,
\end{aligned} \tag{A2}$$

where $\alpha = R/L$ (see, Fig. 1) and ν_0 is the Poissons ratio of the matrix.

APPENDIX B: COMPONENTS OF CONSTITUTIVE STIFFENS TENSOR FOR NANOCOMPOSITES $\chi_{IK}^{(1)}$ AND $\chi_{IJ}^{(2)}$ IN EQ. (10).

$$\begin{aligned}
\chi_{IK}^{(1)} &= 2B_{IK}^{(1)}N_{KK}^{(2)} + 2B_{II}^{(2)}N_{IK}^{(1)} + \sum_{R=1}^{3} B_{IR}^{(1)}N_{RK}^{(1)},\\
\chi_{IJ}^{(2)} &= B_{IJ}^{(2)}N_{IJ}^{(2)} + B_{IJ}^{(2)}N_{JI}^{(2)},
\end{aligned} \tag{B1}$$

in which

$$N_{IK}^{(1)} = -\frac{\Omega_{IK}}{2N_{II}^{(4)}},\quad N_{IJ}^{(2)} = \frac{1}{4N_{II}^{(4)}}, \tag{B2}$$

and

$$\begin{bmatrix}\Omega_{I1}\\ \Omega_{I2}\\ \Omega_{I3}\end{bmatrix} = \begin{bmatrix}N_{11}^{(3)}+2N_{11}^{(4)} & N_{21}^{(3)} & N_{31}^{(3)}\\ N_{12}^{(3)} & N_{22}^{(3)}+2N_{22}^{(4)} & N_{32}^{(3)}\\ N_{13}^{(3)} & N_{23}^{(3)} & N_{33}^{(3)}+2N_{33}^{(4)}\end{bmatrix}^{-1} \cdot \begin{bmatrix}N_{I1}^{(3)}\\ N_{I2}^{(3)}\\ N_{I3}^{(3)}\end{bmatrix}, \tag{B3}$$

[This article is copyrighted as indicated in the article. Reuse of AIP content is subject to the terms at: http://scitation.aip.org/termsconditions. Downloaded to] IP: 143.248.122.51 On: Fri, 18 Jul 2014 14:27:21

with

$$N_{IK}^{(3)} = -2S_{IK}^{(1)}B_{KK}^{(2)} - 2S_{II}^{(2)}B_{IK}^{(1)} - \sum_{R=1}^{3} S_{IR}^{(1)}B_{RK}^{(1)},$$
$$N_{IJ}^{(4)} = \frac{1}{2} - 2S_{IJ}^{(2)}B_{IJ}^{(2)}, \tag{B4}$$

in which

$$B_{IK}^{(1)} = \frac{-\phi_1 T_{IK}}{2\Lambda_{II}^{(2)}}, \quad B_{IJ}^{(2)} = \frac{\phi_1}{4\Lambda_{IJ}^{(2)}}, \tag{B5}$$

with

$$\begin{bmatrix} T_{I1} \\ T_{I2} \\ T_{I3} \end{bmatrix} = \begin{bmatrix} \Lambda_{11}^{(1)} + 2\Lambda_{11}^{(2)} & \Lambda_{21}^{(1)} & \Lambda_{31}^{(1)} \\ \Lambda_{12}^{(1)} & \Lambda_{22}^{(1)} + 2\Lambda_{22}^{(2)} & \Lambda_{32}^{(1)} \\ \Lambda_{13}^{(1)} & \Lambda_{23}^{(1)} & \Lambda_{33}^{(1)} + 2\Lambda_{33}^{(2)} \end{bmatrix}^{-1} \cdot \begin{bmatrix} \Lambda_{I1}^{(1)} \\ \Lambda_{I2}^{(1)} \\ \Lambda_{I3}^{(1)} \end{bmatrix}, \tag{B6}$$

in which

$$\Lambda_{IK}^{(1)} = 2\mu_0\Lambda_{IK}^{(3)} + 2\lambda_0\Lambda_{II}^{(4)} + \lambda_0\left(\sum_{R=1}^{3}\Lambda_{IR}^{(3)}\right) + S_{IK}^{(1)},$$
$$\Lambda_{IJ}^{(2)} = 2\mu_0\Lambda_{IJ}^{(4)} + S_{IJ}^{(2)},$$
$$\Lambda_{IK}^{(3)} = -Y_{IK}/\{2(-\mu_0 + \tilde{\mu}_{II})\},$$
$$\Lambda_{IJ}^{(4)} = 1/\{4(-\mu_0 + \tilde{\mu}_{IJ})\}, \tag{B7}$$

with

$$\begin{bmatrix} Y_{I1} \\ Y_{I2} \\ Y_{I3} \end{bmatrix} = \begin{bmatrix} -\lambda_0 - 2\mu_0 + \tilde{\lambda}_{11} + 2\tilde{\mu}_{11} & -\lambda_0 + \tilde{\lambda}_{21} & -\lambda_0 + \tilde{\lambda}_{31} \\ -\lambda_0 + \tilde{\lambda}_{12} & -\lambda_0 - 2\mu_0 + \tilde{\lambda}_{22} + 2\tilde{\mu}_{22} & -\lambda_0 + \tilde{\lambda}_{32} \\ -\lambda_0 + \tilde{\lambda}_{13} & -\lambda_0 + \tilde{\lambda}_{23} & -\lambda_0 - 2\mu_0 + \tilde{\lambda}_{33} + 2\tilde{\mu}_{33} \end{bmatrix}^{-1} \cdot \begin{bmatrix} -\lambda_0 + \tilde{\lambda}_{I1} \\ -\lambda_0 + \tilde{\lambda}_{I2} \\ -\lambda_0 + \tilde{\lambda}_{I3} \end{bmatrix}, \tag{B8}$$

where λ_0 and μ_0 are the Lamé constants of the matrix material, ϕ_1 is the volume fraction of the CNTs, and $S_{IK}^{(1)}$ and $S_{IJ}^{(2)}$ are the parameters of Eshelby's tensor,[23] which are listed in the Appendix A.

[1]S. Iijima, Nature **354**, 56 (1991).
[2]P. Barai and G. J. Weng, Int. J. Plast. **27**, 539 (2011).
[3]F. T. Fisher, R. R. Bradshaw, and L. C. Brinson, Compos. Sci. Technol. **63**, 1689–1703 (2003).
[4]L. H. Shao, R. Y. Luo, S. L. Bai, and J. Wang, Compos. Struct. **87**, 274 (2009).
[5]R. Tawie, H. K. Lee, and S. H. Park, Smart Struct. Syst. **6**, 851 (2010).
[6]B. J. Yang, H. Shin, H. Kim, and H. K. Lee, Appl. Phys. Lett. **104**, 101901 (2014).
[7]D. L. Shi, X. Q. Feng, Y. Y. Huang, K. C. Hwang, and H. Gao, J. Eng. Mater. Technol **126**, 250 (2004).
[8]V. Anumandla and R. F. Gibson, Composites, Part A **37**, 2178 (2006).
[9]S. Yang, S. Yu, W. Kyoung, D. S. Han, and M. Cho, Polymer **53**, 623 (2012).
[10]B. J. Yang, H. Shin, H. K. Lee, and H. Kim, Appl. Phys. Lett. **103**, 241903 (2013).
[11]H. K. Lee and S. Simunovic, Composites, Part B **31**, 77 (2000).
[12]Z. Liang, H. K. Lee, and W. Suaris, Int. J. Solids Struct. **43**, 5674 (2006).
[13]R. Andrews, D. Jacques, M. Minot, and T. Rantell, Macromol. Mater. Eng. **287**, 395 (2002).
[14]H. M. Hsiao and I. M. Daniel, Compos. Sci. Technol. **56**, 581 (1996).
[15]K. Yanase, S. Moriyama, and J. W. Ju, Acta Mech. **224**, 1351 (2013).
[16]S. Plimpton, J. Comput. Phys. **117**, 1 (1995).
[17]S. J. Stuart, A. B. Tutein, and J. A. Harrison, J. Chem. Phys. **112**, 6472 (2000).
[18]See supplementary material at http://dx.doi.org/10.1063/1.4890519 for the process and results of MS simulations.
[19]K. M. Liew, J. W. Yan, Y. Z. Sun, and L. H. He, Compos. Struct. **93**, 2208 (2011).
[20]H. K. Lee and J. W. Ju, Int. J. Damage Mech. **16**, 331 (2007).
[21]H. K. Lee and S. H. Pyo, Compos. Sci. Technol. **68**, 387 (2008).
[22]J. W. Ju and T. M. Chen, Acta Mech. **103**, 103 (1994).
[23]J. W. Ju and K. Yanase, Int. J. Damage Mech. **18**, 639 (2009).
[24]H. K. Lee and S. Simunovic, Int. J. Solids Struct. **38**, 875 (2000).
[25]B. J. Yang, B. R. Kim, and H. K. Lee, Compos. Struct. **94**, 1420 (2012).

[This article is copyrighted as indicated in the article. Reuse of AIP content is subject to the terms at: http://scitation.aip.org/termsconditions. Downloaded to] IP: 143.248.122.51 On: Fri, 18 Jul 2014 14:27:21